From our findings we conclude that at high magnetic fields the T_1 values of small organotungsten compounds lie in the order of seconds, thus enabling various types of modern one- and two-dimensional NMR pulse experiments to be carried out. Provided that there is a scalar coupling between ^{183}W and both a high γ and a high abundant nucleus (of a few hertz), the two-dimensional indirect ^1H-$\{^{183}W\}$ spectroscopy seems to be the most effective recording technique for determining $\delta(^{183}W)$. In the tris(diene)metal compounds **1-3** (**6-7**) the metal NMR shifts differ significantly. Together with the improved recording conditions it is therefore expected that ^{183}W NMR spectroscopy will become of wider use in organotungsten chemistry.

High-Pressure NMR Studies of CO Exchange with Cobalt Carbonyl Species†

D. Christopher Roe

Central Research & Development Department, E. I. du Pont de Nemours & Company, Experimental Station, Wilmington, Delaware 19898

Received July 15, 1986

Exchange of free CO in solution with $Co_2(CO)_8$ has been studied by ^{13}C magnetization transfer techniques by using a novel high-pressure (sapphire) NMR tube. Rates for CO dissociation were found to be independent of pressure over the pressure and temperature range studied and provide the activation parameters $\Delta H^‡ = 25.5$ kcal/mol and $\Delta S^‡ = 22$ eu. Results obtained for dissociation in CH_3CO–$Co(CO)_4$ suggest stabilization of the coordinatively unsaturated intermediate, possibly by acyl oxygen coordination. Slower scrambling of the acyl CO is also observed and found to be markedly inhibited by higher concentrations of free CO. These results provide the ratio of rates for deinsertion and reassociation in CH_3CO–$Co(CO)_3$.

Introduction

The reactions of organometallic complexes with gases such as H_2 and CO have been of longstanding academic and industrial interest, and of these reactions, cobalt-catalyzed hydroformylation provides a prominent example. Spectroscopic studies in this area have been hampered by the general lack of availability of a cell capable of withstanding the pressures that are required to obtain reasonable concentrations of gas dissolved in solution. While high-pressure IR cells have been fruitfully utilized[1] in this way, the inherent advantages of NMR have remained largely unexploited because of the demands associated with construction and operation of high-pressure NMR probes.[2,3]

We have recently developed a high-pressure NMR tube, which is convenient to use, is relatively inexpensive and is suitable for use in commercial spectrometers without probe or hardware modification. In contrast to high-pressure IR cells, which require their own temperature control mechanism, this tube can directly take advantage of the full variable-temperature capabilities of NMR spectrometers (e.g., -100 to +150 °C). Finally, the new tube permits for pressurized samples the general advantage of NMR—namely, a direct basis for the determination of concentrations and the identification of chemical species.

While details of construction and performance of this high-pressure NMR tube have been presented elsewhere,[4] a brief description is included here. The tube consists of a single crystal of sapphire that was grown to the required dimensions (5-mm o.d. with 0.8-mm wall) and is sealed by means of a nonmagnetic titanium alloy valve. The tubes spin, provide routine resolution of approximately 1 Hz, and appear to offer a reasonable margin of safety in operation up to 2000 psi.

Caution: Although the burst pressure was found, in *one* test, to be in excess of 10 000 psi, it is impossible to specify a safe upper pressure limit with any accuracy. The detailed history of a given tube may eventually affect its performance. Pressurized tubes should always be transported behind an appropriate safety shield, and direct operator exposure to the tube must be avoided. Being single crystalline in nature, the tubes may be sensitive to vibrations such as occur in an ultrasonic cleaning bath.

The availability of these high-pressure tubes facilitates the systematic variation of dissolved gas concentrations in kinetic studies and also provides a means for stabilizing labile transition-metal carbonyl species. Both of these considerations apply to the current study that presents the details of our ^{13}C NMR investigations of CO exchange involving $Co_2(CO)_8$ and the model acyl CH_3CO–$Co(CO)_4$. The exchange processes involved are fundamental in the context of providing coordinatively unsaturated intermediates for the oxidative addition of H_2 or for reaction with other species.

Results

Exchange Involving $Co_2(CO)_8$. At pressures between 100 and 1100 psig of ^{13}CO, cyclohexane-d_{12} solutions of $Co_2(CO)_8$ reveal ^{13}C NMR spectra containing separate peaks for free CO and universally enriched $Co_2(CO)_8$ as the only species observable (see Figure 1). Since intramolecular exchange of the CO groups in $Co_2(CO)_8$ is very rapid,[5,6] all the coordinated CO's are treated as being equivalent. Although the use of ^{13}C-enriched CO is not

† Contribution No. 3670.

(1) (a) Mirbach, M. F. *J. Organomet. Chem.* **1984**, *265*, 205-213. (b) Mirbach, M. J.; Mirbach, M. F.; Saus, A.; Topalsavoglou, N.; Phu, T. N. *J. Am. Chem. Soc.* **1981**, *103*, 7590-7594.
(2) Pisaniello, D. L.; Helm, L.; Meier, P.; Merbach, A. E. *J. Am. Chem. Soc.* **1983**, *105*, 4528-4536.
(3) Jonas, J.; Hasha, D. L.; Lamb, W. J.; Hoffman, G. A.; Eguchi, T. *J. Magn. Reson.* **1981**, *42*, 169-172.
(4) Roe, D. C. *J. Magn. Reson.* **1985**, *63*, 388-391.
(5) Todd, L. J.; Wilkinson, J. R. *J. Organomet. Chem.* **1974**, *77*, 1-25.
(6) Absi-Halabi, M.; Atwood, J. D.; Forbus, N. P.; Brown, T. L. *J. Am. Chem. Soc.* **1980**, *102*, 6248-6254.

0276-7333/87/2306-0942$01.50/0

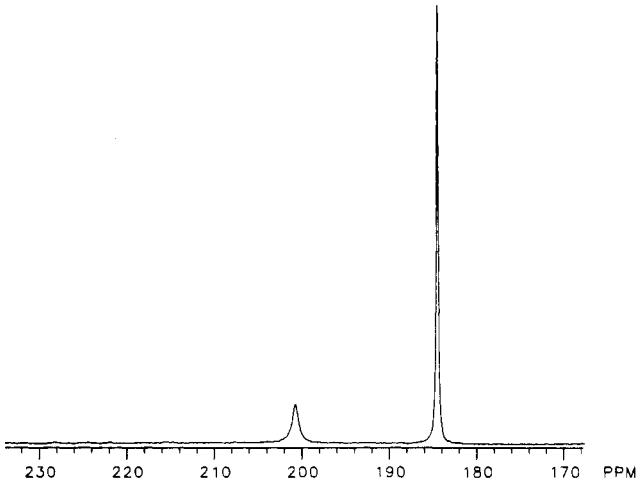

Figure 1. ^{13}C NMR spectrum of $Co_2(CO)_8$ (200.56 ppm) and free CO (184.56 ppm) obtained at 1100 psig of CO in C_6D_{12} (80 °C). The concentration of free CO is estimated to be 1.43 M.

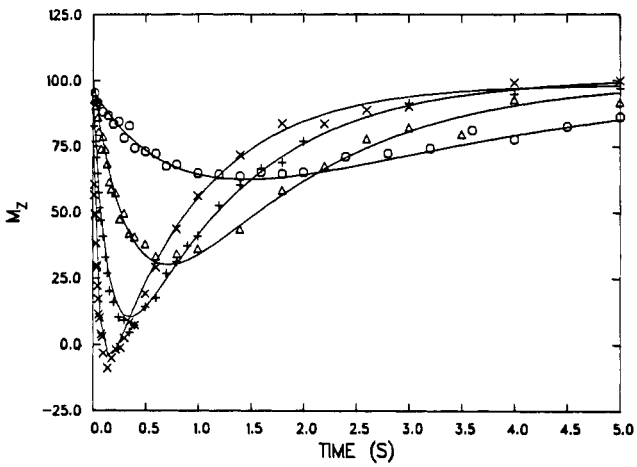

Figure 2. Response of $Co_2(CO)_8$ signal (M_z) to selective inversion of free CO at 50 (○), 60 (△), 70 (+), and 80 °C (×). Solid curves represent the best fit to combined data sets (inverted CO, $Co_2(CO)_8$ response; inverted $Co_2(CO)_8$, CO response) at each temperature. Data from 40 °C are omitted for clarity.

a prerequisite for the observation of ^{13}C signals in the sapphire tube, it does provide an important improvement in signal-to-noise for the work reported here since the the experiments rely on the potentially long ^{13}C T_1's in the cobalt complexes.

Under the conditions described above, the concentration of CO in solution varies from approximately 0.08 to 1.43 M ($Co_2(CO)_8$ is estimated to be 5.8×10^{-2} M). Spectra obtained between 40 and 80 °C show that the two species are exchanging slowly on the NMR time scale, and this exchange can be followed by magnetization transfer techniques. Line widths for $Co_2(CO)_8$ vary from 35 at 30 °C to 75 Hz at 80 °C; however, line-shape information at these temperatures is complicated by broadening attributed to the quadrupolar cobalt nucleus. Since the extent of the quadrupolar broadening is significant (ca. 50% of the observed linewidth) and is expected to increase at higher temperatures, complete line-shape analysis was not pursued.

A typical magnetization transfer experiment consists of selective inversion of one resonance followed by a variable time delay and signal acquisition (see Figure 2); the complementary experiment involving selective inversion of the other resonance is also performed, and the combined data sets are analyzed to provide a single consistent rate constant along with estimates of the individual site T_1's.

Table I. Exchange Rate and Relaxation Parameters for CO Dissociation in $Co_2(CO)_8$[a]

T, °C	k_1, s^{-1}	T_1, s	
		CO	$Co_2(CO)_8$
40	0.78 (0.02)	1.0	10.1
50	3.06 (0.05)	1.0	6.7
60	11.36 (0.16)	0.9	7.8
70	32.48 (0.56)	0.9	1.7
80	93.60 (2.24)	0.9	1.1

[a] Standard deviation in parentheses. T_1 values are considered accurate to no better than 10%.

Experiments at three of four different CO pressures were performed at each temperature, and the rate constants were found to exhibit no apparent trend with respect to CO concentration. The different rate determinations at a given temperature agreed within 10–15%, and the associated standard errors (provided by the analysis) were used to calculate the weighted average rate constants and standard deviations reported in Table I. The independence of the observed exchange rate on CO concentration is consistent with the small value ($\sim 10^{-4}$ M^{-1})[7,8] of the equilibrium dissociation constant, and thus the observed rates correspond directly to k_1 (eq 1). The rate constants of Table I lead to the activation parameters $\Delta H^{\ddagger}$ = 25.5 (1.5) kcal/mol and $\Delta S^{\ddagger}$ = 22 (4) eu; $\Delta G^{\ddagger}$(300 K) = 18.8 (0.2) kcal/mol.

$$Co_2(CO)_8 \underset{k_{-1}}{\overset{k_1}{\rightleftharpoons}} Co_2(CO)_7 + CO \qquad (1)$$

Since dilution of the cobalt solution from 5.8×10^{-2} to 2.3×10^{-2} M has no effect on the rate (at the lower concentration, $k_1 = 10.88 \pm 0.40$ s^{-1} at 60 °C), it is inferred that $Co(CO)_4$ radicals are not involved in the exchange under the mild conditions of these experiments.

Exchange Involving CH_3CO–$Co(CO)_4$. Solutions of CH_3CO–$Co(CO)_4$ were obtained by extracting the appropriate reaction mixture below 0 °C using small amounts of methylcyclohexane-d_{14}. Incorporation of ^{13}CO was found to proceed overnight at 0 °C, whereas the equilibrium distribution of labeled CO was typically achieved within an hour or two at 30 °C. It was found that under high-pressure conditions (1000 psig at room temperature) the sample of CH_3CO–$Co(CO)_4$ appeared to be stable for hours at 100 °C, while at lower pressure (100 psig) the sample remained unchanged after a period of 2 months at room temperature.

Magnetization transfer experiments at 50 °C revealed exchange between the terminally bonded CO ligands on cobalt and free CO in solution, while at higher temperatures an additional slower scrambling of the acyl carbonyl was also observed (see Figure 3). Quantitative experiments were most effectively initiated by means of a "selective" 180° pulse centered on the $Co(CO)_4$ resonance even though this pulse also perturbed the intensity of the small $Co_2(CO)_8$ signal which was unavoidably present. The exchange model therefore included eq 1 in addition to eq 2 and 3 and thus expanded the analysis to one involving

$$CH_3CO\text{–}Co(CO)_4 \underset{k_{-2}}{\overset{k_2}{\rightleftharpoons}} CH_3CO\text{–}Co(CO)_3 + CO \qquad (2)$$

$$CH_3CO\text{–}Co(CO)_3 \underset{k_{-3}}{\overset{k_3}{\rightleftharpoons}} CH_3\text{–}Co(CO)_4 \qquad (3)$$

four sites and three exchange rates. The estimates of k_1

(7) Ungvary, F. *J. Organomet. Chem.* **1972**, *36*, 363–370.
(8) Ungvary, F.; Marko, L. *J. Organomet. Chem.* **1974**, *71*, 283–286.

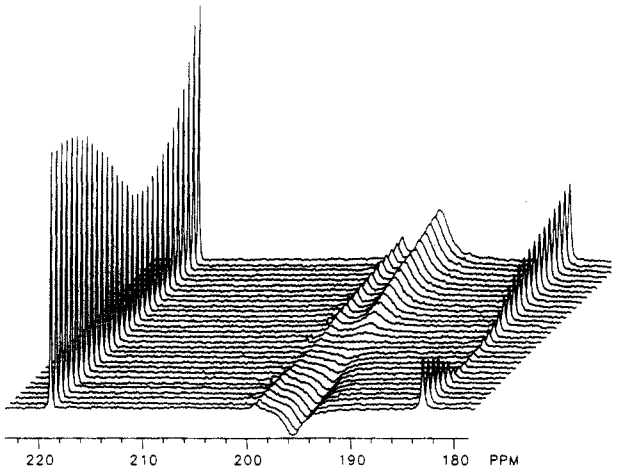

Figure 3. Observed ^{13}C NMR spectral response to selective inversion of the $Co(CO)_4$ signal (197.09 ppm) in methylcyclohexane-d_{14} at 70 °C. The concentration of free CO is approximately 0.42 M.

Table II. Exchange Rates for CO Dissociation and Acyl CO Scrambling in CH_3CO-$Co(CO)_4$[a]

		k_{acyl}, s^{-1}		
T, °C	k_2, s^{-1}	A[b]	B	C
50	0.57 (0.11)	0.026 (0.009)	0.027 (0.006)	
60	1.65 (0.31)	0.112 (0.016)	0.076 (0.025)	
70	4.49 (0.23)	0.413 (0.026)	0.312 (0.044)	0.139 (0.028)
80	11.46 (0.78)		0.940 (0.089)	0.473 (0.058)

[a] Numbers in parentheses represent one standard deviation. [b] CO concentration = 0.42 (A), 0.60 (B), and 1.43 M (C).

provided by this four-site analysis were entirely consistent with those reported in Table I but were considerably less precise.

Exchange between free CO and the cobalt tetracarbonyl fragment was found to be independent of the concentration of dissolved CO, just as had been observed for $Co_2(CO)_8$. The equilibrium constant for CO dissociation must be considerably smaller than the concentrations of species present under our particular set of conditions and might therefore be similar to that for $Co_2(CO)_8$. The exchange rates determined must then correspond directly to k_2, and the average values from different runs are reported in Table II (results from a typical analysis are displayed in Figure 4).

It may be noted that the results for k_2 are neither as extensive nor as accurate as the k_1 values reported for CO dissociation from $Co_2(CO)_8$ in Table I; the exchange is inherently slower for CH_3CO-$Co(CO)_4$ and cannot be followed by magnetization transfer below 50 °C, while the presence of the $Co_2(CO)_8$ impurity and the multisite nature of the problem make experiments above 80 °C impractical. Another feature that limits the quality of the rate determinations is the extent to which the T_1's differ between sites (e.g., at 70 °C, T_1 for the $Co(CO)_4$ carbons is 13 s while the acyl carbonyl carbon has a T_1 of approximately 30 s—cf. Table I). In this circumstance the balance between exchange and relaxation rates cannot be maintained for all sites, particularly at the higher temperatures, and the T_1's for the noninverted sites tend to be poorly determined. Nevertheless, the dissociation rate constants (k_2) presented in Table II for CH_3CO-$Co(CO)_4$ lead to the activation parameters $\Delta H^{\ddagger}$ = 22.0 (0.2) kcal/mol, $\Delta S^{\ddagger}$ = 8 (0.5) eu, and $\Delta G^{\ddagger}$(300 K) = 19.5 (0.02) kcal/mol.

The scrambling of the acyl with the terminal CO's is most reasonably presumed to occur by the deinsertion process described by eq 3. The rate of acyl exchange is

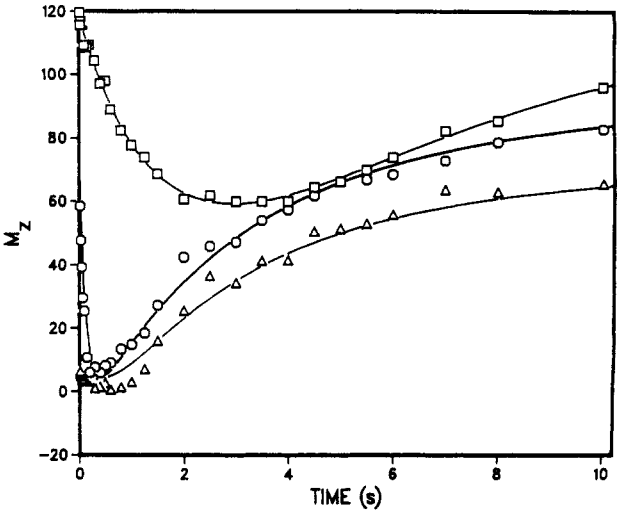

Figure 4. Response of free CO (○), acetyl CO (□), and $Co_2(CO)_8$ (△) to selective inversion of the $Co(CO)_4$ signal (conditions specified in Figure 3). The solid curves represent the best fit to the four-site model (see Experimental Section). Data were acquired up to delays of 20 s.

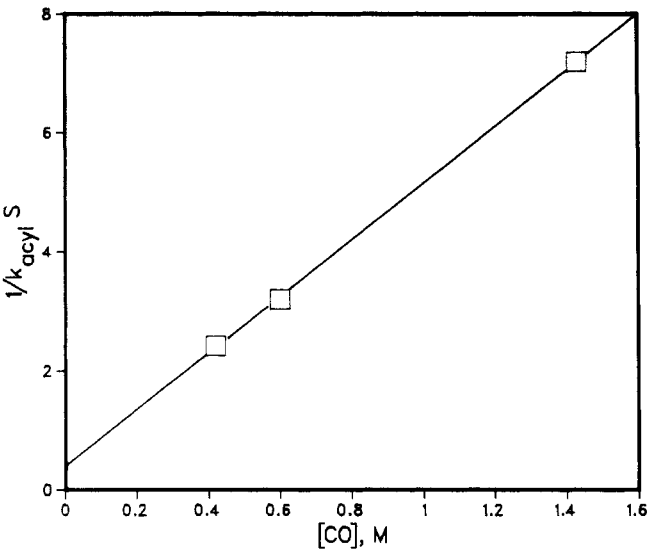

Figure 5. Plot of $1/k_{acyl}$ vs. CO concentration.

markedly inhibited by increasing the CO pressure and thereby decreasing the lifetime of the coordinatively unsaturated intermediate (reverse of eq 2). A simple interpretation of the observed exchange rate k_{acyl} is only available if it can be assumed that $k_{-3} \ll k_3$. If the assumption is valid, then the steady-state condition yields eq 4, and a plot of $1/k_{acyl}$ vs. CO concentration should

$$k_{acyl} = \frac{k_2 k_3}{k_{-2}[CO] + k_3} \tag{4}$$

provide a straight line with intercept $1/k_2$ and slope $k_{-2}/(k_2 k_3)$. That k_{-3} is indeed insignificant compared to k_3 is suggested by the plot in Figure 5; the intercept provides an independent estimate for k_2 = 2.5 s^{-1} at 70 °C that is in rough agreement with the more accurate magnetization transfer data. With use of the latter value for k_2, the ratio of the rates of reassociation to deinsertion (i.e., $k_{-2}[CO]/k_3$) can be estimated from the slope, and for [CO] = 1.0 M at 70 °C, this ratio is approximately 21.

Discussion

Dissociation of CO from either $Co_2(CO)_8$ or coordinatively saturated Co acyl complexes (RCO-$Co(CO)_4$) is

almost universally cited as the source of CO inhibition in the kinetics of subsequent reactions with, for example, H_2 or $HCo(CO)_4$, and rate constants for dissociation have be estimated from such kinetics.[7] The high-pressure NMR tubes described in this paper provide a means for directly monitoring these fundamental dissociation rates under conditions which are closely related to those in the hydroformylation process, and have also provided insight to the reassociation and insertion/deinsertion steps.

Earlier attempts to measure directly the exchange of CO with $Co_2(CO)_8$ involved either monitoring gas-phase levels of ^{14}CO radioactivity above solutions of $Co_2(CO)_8$ from −20 to +5 °C[9] or following IR changes during the incorporation of ^{13}CO at 0 °C.[6] Although the IR approach is, in principle, inherently direct and accurate, the experimental uncertainties in the rate determination just cited were still quite large (approximately 30%). However, substitution of CO by $AsPh_3$ (presumed to occur by rate-limiting dissociation from $Co_2(CO)_8$) could be studied from −15 to +30 °C,[6] and these rates led to the activation parameters $\Delta H^\ddagger$ = 22.2 kcal/mol and $\Delta S^\ddagger$ = 10 eu.

The sapphire NMR tubes are seen to facilitate the study of $Co_2(CO)_8$ while the concentration of CO in solution is systematically varied. The NMR techniques described above provide a means for evaluating the dissociation rate as a simple two-site exchange problem, and the temperature range over which the magnetization transfer methods are applicable is sufficient for the determination of reasonably accurate activation parameters. Line-shape changes at higher temperatures are complicated by the quadrupolar cobalt nucleus in that the ^{13}C line widths would be expected to increase with the cobalt T_1 (i.e., even in the absence of exchange). A "partial" line-shape analysis involving the line width of the free CO alone is consistent with the magnetization transfer results above 60 °C; for example, at 80 °C the free CO line width leads to an estimate for $k_1 = 97\ s^{-1}$. However, the magnetization transfer method is preferred in general because fitting a time-dependent curve is inherently more accurate than a single line-width measurement and because error estimates are obtained directly from the analysis.

Dissociation from $CH_3CO–Co(CO)_4$ can be followed similarly but is complicated by the multisite nature of the problem and the range of T_1 values encountered for the different sites (as described above). Nevertheless, the activation parameters determined compare favorably with those reported[10] recently from IR kinetic studies of the decomposition of *n*-butyryl- and isobutyrylcobalt tetracarbonyl (e.g., $\Delta H^\ddagger$ = 19.6 kcal/mol and $\Delta S^\ddagger$ = 0.1 eu).

Notable differences exist in the comparison of activation parameters for CO dissociation in $Co_2(CO)_8$ and $CH_3CO–Co(CO)_4$. Although the dissociation rate from $Co_2(CO)_8$ is several times faster in the temperature range studied, the enthalpy of activation is some 3.5 kcal/mol higher, and the faster rate is due to the substantially larger $\Delta S^\ddagger$. While the large positive $\Delta S^\ddagger$ is consistent with a dissociative process for $Co_2(CO)_8$, the small $\Delta S^\ddagger$ for the analogous process in $CH_3CO–Co(CO)_4$ suggests a marked difference between the two transition states. It is inferred that the transition state for CO dissociation in $Co_2(CO)_8$ does not involve an increase in structure, whereas the loss of CO in $CH_3CO–Co(CO)_4$ is accompanied by a stabilizing coordination of the acyl oxygen. The kinetic results therefore are in accord with the structures inferred[11] for the unsaturated intermediates in matrix isolation FT-IR studies of photochemically generated $Co_2(CO)_7$ and $CH_3CO–Co(CO)_3$.[11]

The kinetics of acyl exchange (as studied by this method) do not allow the evaluation of specific rate constants but rather give the ratio of rates for the first-order deinsertion step to the second-order reassociation back to $CH_3CO–Co(CO)_4$; thus the CO concentration needs to be specified in comparing the relative rates. From the limited data available in Table II, it may be perceived that increasing the temperature tends to involve a more rapid increase in the rate of deinsertion compared to the rate of reassociation, as would be expected for a comparison of first- and second-order processes. Roughly speaking, under the present conditions of temperature and CO concentration, reassociation to give the acyl is inherently about 20 times faster than deinsertion to give the alkyl.

In addition to the above studies, it has been found possible to follow the production of $HCo(CO)_4$ in C_6D_{12} solution using 500–1000 psi of CO/H_2 in the same pressure tubes and to demonstrate the inhibitory effect of CO on both the formation and decomposition of $HCo(CO)_4$. While quantitative NMR investigation of these steps can now be readily accomplished, the sapphire tubes should be generally useful for those studies that benefit from high concentrations of dissolved gas.

Experimental Section

General Data. Sample preparations were carried out in a Vacuum Atmospheres drybox, and deuteriated solvents (Merck) were dried and degassed prior to use. Dicobalt octacarbonyl (Pressure Chemical) was obtained as pale orange crystals by recrystallization from pentane. Sodium tetracarbonylcobaltate was prepared from $Co_2(CO)_8$ according to the literature method.[12] Acetylcobalt tetracarbonyl was prepared by the reaction of Na[$Co(CO)_4$] with MeI in the presence of CO.[13]

NMR spectra were recorded by using a Nicolet NT-360 WB spectrometer operating at 360.905 MHz for ^1H and 90.759 MHz for ^{13}C. ^{13}CO chemical shifts (referenced to external Me_4Si) observed at 50 °C: $Co_2(CO)_8$, δ 201.28; $CH_3CO–Co$, δ 219.07; $Co(CO)_4$, δ 196.13; free CO, δ 183.58.

NMR solutions of $Co_2(CO)_8$ were simply obtained by dissolving a weighed amount of the crystalline material in a known volume of deuteriated solvent and syringing the solution into the sapphire tube. Since the cobalt complex appeared to dissolve entirely, the concentrations of free CO in solution were approximated from the integrated ^{13}C NMR intensities. The degree of ^{13}C enrichment in individual samples varies according to the pressure of ^{13}CO used to charge the tube and to the amount of cobalt complex being exposed to labeled CO. However, the equilibrium distribution of ^{12}CO and ^{13}CO is readily achieved on the "chemical time scale" both for the cobalt complex and for the free CO, and since the result is a uniformly enriched system, the observed ^{13}C NMR peak areas directly reflect the concentrations of species in solution. Solutions of $CH_3CO–Co(CO)_4$ were obtained by extracting the contents of the reaction flask with small volumes of methylcyclohexane-d_{14} at the lowest temperature consistent with the apparent solubility of the complex. The solution was transferred via cold syringe to the sapphire tube kept at dry ice temperature.

Once the tube had been sealed by means of the titanium alloy valve, it was removed from the drybox, transported inside a safety shield, and pressurized with 99% ^{13}CO (Isotec). Dissolution of the gas was achieved by gently rocking the tube assembly on its side several times. In the case of $CH_3CO–Co(CO)_4$, the tube was

(9) Breitschaft, S.; Basolo, F. *J. Am. Chem. Soc.* **1966**, *88*, 2702–2706.
(10) Kovacs, I.; Ungvary, F.; Marko, L. *Organometallics* **1986**, *5*, 209–215.
(11) Evidence that the carbonyl group in $CH_3CO–Co(CO)_3$ is bonded in an η^2 fashion has been obtained. Sweany, R., private communication: Sweany, R. L.; Russell, F. N., submitted for publication in *J. Am. Chem Soc.*
(12) Edgell, W. F.; Lyford, J. *Inorg. Chem.* **1970**, *9*, 1932–1933.
(13) Heck, R. F.; Breslow, D. S. *J. Am. Chem. Soc.* **1962**, *84*, 2499–2502.

only then allowed to come to room temperature.

Magnetization Transfer Experiments. Estimates of the ^{13}C site T_1's were obtained by standard inversion-recovery techniques using a composite 180° pulse and a three-parameter fit to the data. The T_1 values obtained at the lowest temperature that exchange could be detected were used as initial guesses in the magnetization transfer analysis and were at least consistent with T_1 measurements made at higher temperatures. The long T_1 of the acyl carbon necessitated a recycle delay of 150 s for the experiments involving CH_3CO–$Co(CO)_4$, and between 16 and 32 accumulations were acquired for each time point in a given experiment. Magnetization transfer experiments were initiated by a selective inversion pulse arranged to be between 1 and 6 ms by attenuation of the low power transmitter; spectra were acquired as a function of time from 20 ms up to 50 s following the initial perturbation. The time dependence of the integrated areas was obtained from standard Nicolet software, and these experimental intensities used as input for a general multisite analysis.

The evaluation of exchange and relaxation rate constants in an n-site system depends on the time evolution of z magnetization according to a set of coupled differential equations (eq 5), where

$$d\mathbf{M}(t)/dt = (\mathbf{K} + \mathbf{R})\Delta\mathbf{M}(t) \quad (5)$$

$\Delta\mathbf{M}(t) = (\mathbf{M}(t) - \mathbf{M}^{eq})$ is an n vector of deviations of the (n) z magnetizations ($\mathbf{M}(t)$) from thermal equilibrium ($\mathbf{M}^{eq}$). The diagonal relaxation matrix $\mathbf{R}$ contains the relaxation rate constants written as $-(1/T_1)_i$ for the individual sites, while the exchange matrix $\mathbf{K}$ contains terms K_{ij} describing the rate of transfer from site j to site i (the diagonal terms $-K_{ii}$ describe the loss of magnetization from site i to the other sites). The formal solution of eq 5 is expressed in terms of the diagonal matrix $\mathbf{D}$ (containing the eigenvalues $-\lambda_i$)

$$\mathbf{D} = \mathbf{T}^{-1}(\mathbf{K} + \mathbf{R})\mathbf{T} \quad (6)$$

where the diagonalizing matrix $\mathbf{T}$ is found by standard numerical procedures (our particular implementation involved the EISPACK routines). The time dependence of the z magnetization is then given by eq 7, where $\mathbf{M}(0)$ describes the initial ($t = 0$) site intensities. Best guesses for the initial and equilibrium magnetizations, the T_1's, and the rate constants are iteratively adjusted to provide both the least-squares best fit to the experimental observations and the standard deviations for the parameter estimates.

$$\mathbf{M}(t) = \mathbf{T}(\exp-\mathbf{D}t)\mathbf{T}^{-1}(\mathbf{M}(0) - \mathbf{M}^{eq}) + \mathbf{M}^{eq} \quad (7)$$

The two-site exchange of CO with $Co_2(CO)_8$ is particularly simple and would not by itself require the general treatment given above (analytic solutions are available and have been presented by others[14,15]). The exchange processes involved in the CH_3C-O–$Co(CO)_4$ experiments are assumed to be described by eq 2 and 3 (i.e., there is no direct pathway for exchanging the acyl with free CO etc.), and include eq 1 because of the $Co_2(CO)_8$ impurity present. The sites are labeled 1 ($Co(CO)_4$), 2 (CH_3CO–), 3 (free CO), and 4 ($Co_2(CO)_8$); the required equilibrium ratios are $A = M^{eq}{}_1/M^{eq}{}_3$ and $B = M^{eq}{}_4/M^{eq}{}_3$. Making the identifications with the rate constants described in the Results, the exchange matrix $\mathbf{K}$ becomes eq 8. Since the exchange and relaxation rates involving $Co_2(CO)_8$ were well-determined in the first set of experiments, it is unimportant that the "selective" inversion pulse on the $Co(CO)_4$ resonance partly perturbs the $Co_2(CO)_8$ signal; the initial intensity ($\mathbf{M}_4(0)$) is simply another parameter in the fit, and the exchange contribution from k_1 is readily estimated.

$$\mathbf{K} = \begin{pmatrix} -k_{acyl}/4 - k_2/4 & k_{acyl}A & k_2A/4 & 0 \\ k_{acyl}/4 & -k_{acyl}A & 0 & 0 \\ k_2/4 & 0 & -k_2A/4 - k_1B/8 & k_1/8 \\ 0 & 0 & k_1B/8 & -k_1/8 \end{pmatrix} \quad (8)$$

The activation parameters reported for the dissociation rate constants were determined by fitting the results to the Eyring equation by using a nonlinear least-squares program and assuming a 10% error in the absolute rate constant and a 2 °C error in the temperature. The error estimates in the activation parameters represent 95% confidence limits.

Acknowledgment. I am indebted to Prof. Alan D. King, Jr. (University of Georgia), for suggesting the possible use of sapphire tubes and to O. R. Van Buskirk (Experimental Station) and his staff for engineering assistance. I also thank Prof. Ray L. Sweany for communicating results prior to publication, E. A. Conaway for fine technical assistance, and Dr. R. T. Baker for preparation of the cobalt complexes.

(14) Alger, J. R.; Prestegard, J. H. *J. Magn. Reson.* **1977**, *27*, 137-141.
(15) Led, J. J.; Gesmar, H. *J. Magn. Reson.* **1982**, *49*, 444-463.

Some Platinum(II) and Iridium(III) Complexes with Direct Mercury–Hydrogen Bonds

Brian S. McGilligan, Luigi M. Venanzi,* and Martin Wolfer

Laboratorium für Anorganische Chemie, ETH, CH-8092 Zürich, Switzerland

Received September 17, 1986

The preparation in solution and the NMR characterization of complexes of the types $[L_2(C_6Cl_5)Pt(\mu\text{-}H)HgR](CF_3SO_3)$ (for L = PEt_3, R = n-$C_{12}H_{25}$, $PhCH_2$, 2,4,6-$Me_3C_6H_2$, Ph, 4-ClC_6H_4; for L = PMe_3, R = $PhCH_2$, 2,4,6$Me_3C_6H_2$, Ph) and $[(triphos)(H_{3-x})Ir(\mu\text{-}H)_xHgR](CF_3SO_3)$ (triphos = $CH_3C(CH_2PPh_2)_3$, R = n-$C_{12}H_{25}$, $PhCH_2$, 2,4,6-$Me_3C_6H_2$, Ph, 4-ClC_6H_4, 2,4,6-$Cl_3C_6H_2$) are described. The values of the $^1J(^{199}Hg, ^1H)$ coupling constants range from 600 to 1000 Hz for the former class of compounds and from 126 to 475 Hz for the latter class of compounds. Although some of these species can be obtained in the solid state by low-temperature precipitation and can be stored indefinitely at ca. −20 °C, their solutions decompose above ca. −30 °C for the platinum complexes and ca. −60 °C for the iridium complexes.

Introduction

Many attempts have been made to prepare compounds containing mercury–hydrogen bonds. Thus Wiberg and Henle[1] describe the synthesis of HgH_2 and report that it decomposes above −125 °C.

Much work has also been done on the reductive demercuration of alkyl- and arylmercury halides[2-6] by main-

(1) Wiberg, E.; Henle, W. *Z. Naturforsch. B: Anorg. Chem., Org. Chem., Biochem., Biophys., Biol.* **1951**, *6B*, 461.
(2) Whitesides, G. M.; San Filippo, J., Jr. *J. Am. Chem. Soc.* **1970**, *92*, 6611.
(3) Perié, J. J.; Lattes, A. *Bull. Soc. Chim. Fr.* **1971**, 1378.
(4) Hill, C. L.; Whitesides, G. M. *J. Am. Chem. Soc.* **1974**, *96*, 870.
(5) Quirk, R. P.; Lea, R. E. *J. Am. Chem. Soc.* **1976**, *98*, 5973.

0276-7333/87/2306-0946$01.50/0